



Article

Defining the Effect of a Polymeric Compatibilizer on the Properties of Random Polypropylene/Glass Fibre Composites

Evangelia Delli ^{1,*}, Dimitrios Gkiliopoulos ², Evangelia Vouvoudi ³, Dimitrios Bikiaris ^{3,*}
and Konstantinos Chrissafis ¹

¹ Laboratory of Advanced Materials and Devices, Department of Physics, Aristotle University of Thessaloniki, GR-541 24 Thessaloniki, Greece; hrisafis@physics.auth.gr

² Laboratory of Chemical and Environmental Technology, Department of Chemistry, Aristotle University of Thessaloniki, GR-541 24 Thessaloniki, Greece; dgiliopo@chem.auth.gr

³ Laboratory of Polymer Chemistry and Technology, Department of Chemistry, Aristotle University of Thessaloniki, GR-541 24 Thessaloniki, Greece; evouvoud@chem.auth.gr

* Correspondence: evdelli@physics.auth.gr (E.D.); dbic@chem.auth.gr (D.B.)

Abstract: Random polypropylene composites reinforced with short glass fibres have been successfully fabricated by melt-mixing. Polypropylene grafted with maleic anhydride (PP-g-MA) was added to the composites, which was expected to act as a compatibilizer and greatly limit the negative effects known to arise from the feeble polymer matrix/glass fibre interfaces. The effect of compatibilizer concentration on the structural, mechanical and thermal behaviour of the composites has been investigated. The results revealed an improvement of the glass fibre/matrix interaction upon the addition of the compatibilizer, which resulted in enhancing the overall material stiffness and the ability of the matrix to store energy. In particular, the lowering of the glass transition and the investigation of the fracture surfaces of the composites confirmed the improved PP_R/fibre adhesion. Examination of the tensile elongation indicated the improvement of the Young's modulus and yield strength with the addition of PP-g-MA, while the storage modulus was also shown to be significantly increased. These results confirmed the versatility and efficiency of the approach presented in this work to improve the thermomechanical properties and sustainability of PP_R and promote its usage in industrial applications and commercial manufacturing.

Keywords: polypropylene composites; glass fibres; chemically modified polypropylene; maleic anhydride; mechanical properties



Citation: Delli, E.; Gkiliopoulos, D.; Vouvoudi, E.; Bikiaris, D.; Chrissafis, K. Defining the Effect of a Polymeric Compatibilizer on the Properties of Random Polypropylene/Glass Fibre Composites. *J. Compos. Sci.* **2024**, *8*, 44. <https://doi.org/10.3390/jcs8020044>

Academic Editor: Francesco Tornabene

Received: 22 December 2023

Revised: 15 January 2024

Accepted: 23 January 2024

Published: 25 January 2024



Copyright: © 2024 by the authors. Licensee MDPI, Basel, Switzerland. This article is an open access article distributed under the terms and conditions of the Creative Commons Attribution (CC BY) license (<https://creativecommons.org/licenses/by/4.0/>).

1. Introduction

The formation of reinforced thermoplastic composites has allowed the development of advanced polymeric materials with improved damage tolerance, high rigidity, fatigue endurance and environmental resistance. One approach to enhance the resistance, modulus and mechanical properties of thermoplastics is to incorporate high-performance organic and/or inorganic fibres. Glass fibres (GFs) are often chosen in industry [1] as a reinforcing agent due to their incomparable high strength-to-weight ratio efficacy and stiffness. Additionally, due to the low raw-material cost of GFs compared to other commercial additives such as clays and carbon nanotubes [2], as well as their high recycling potential [3], the industrial usage and mass production of the GF composites is feasible. However, the efficiency of reinforcement and the final performance of glass fibre composites is strongly affected by the interfacial adhesion force between the polymer matrix and the surface of the fibres. Poor matrix–fibre bonding, as a result of the high surface energy of the fibres and the low matrix wettability/hydrophobicity, leads to highly defected composites with low mechanical strength, since stress transferring from the polymeric matrix to the fibrous reinforcing agent cannot be sufficiently achieved. Of all classes of polymers, polyolefins are the hardest to be combined with other materials, even organic substances, due to the

lack of functional groups for bonding or even affinity. Organofunctional silane coating, commonly known as sizing, is often applied to the surface of the fibres to promote interfacial adhesion [4] via the formation of covalent bonds [5]. Furthermore, it was reported previously that the incorporation of polar functional groups in the polymer chain such as such as grafted maleic anhydride [6] improves the interfacial adhesion in composites and promotes the homogenous dispersion of the reinforcing agent. The anhydride groups of the grafted polyolefin compatibilizers chemically react with the amino groups of fibre sizing (coating), which remarkably enhances the fibre/matrix interaction [7], leading to strengthened composites [8]. Free-radical grafting of maleic acid onto polymer blends has gained acceptance since maleic-acid-grafted polyolefins were found to exhibit high compatibility, *pe*.for combining LDPE and PVA [9].

Polypropylene (PP) is classified among the most commercially used polyolefins, with applications in industrial fields such as packaging, electrical manufacturing and household appliances, mainly due to its easy processability, good chemical and moisture resistance and high flexural strength. These properties also make PP a candidate matrix material for composites. However, the characteristic low impact resistance, poor dimensional stability and relatively low maximum service temperature often limit its suitability for highly demanding applications. Copolymerization of PP with small volumes of different olefin monomers has been seen to greatly benefit the impact strength [10,11] and the thermal properties of polypropylene [12]. Thus, random polypropylene (PP_R) contains up to 10 wt.% ethylene units randomly dispersed into the PP matrix and exhibits high elasticity, good impact and creep resistance and increased longevity. Furthermore, the embedded ethylene units strongly affect the crystalline/amorphous ratio of the blend, which determines the stiffness of the material [13]. It was reported previously that incorporation of 10 wt.% short glass fibres in the random polypropylene matrix greatly enhances the strength and modulus of elasticity of the matrix [14], making PP_R/GF composites suitable for structural engineering applications such as chemical media piping, heating and water supply systems, as PP and PE are the key polymers in pipe manufacturing of all purposes. It was also shown that further increase in the fibre content significantly lowers the tensile performance. However, not much work has been focused on the effect of compatibilizers on the mechanical and thermal properties of glass-fibre-reinforced PP_R. The novelty of this piece of work is that the role of the compatibilizer is under investigation by applying most of the characterization techniques that concern PP.

In this work, 10 wt.% short-glass-fibre-reinforced PP_R composites were obtained by melt-mixing using silane-sized GFs and PP-g-MA as the compatibilizing agent. Different amounts of PP-g-MA were used to demonstrate the effect of compatibilizer loading on the interfacial adhesion and the physical characteristics of the PP_R/GF composites. The impact of the compatibilizer on the crystallization behaviour, the adhesion and the mechanical properties of the composites was investigated. It is anticipated that the enhancement of the mechanical and thermal properties of the PP-g-MA modified PP/GF composites will facilitate the design of high-performance and -durability heating pipeline systems.

2. Materials and Methods

2.1. Materials

The PP_R material with a density of approximately 0.85 g/cm³ was kindly provided by Interplast S.A. "E-glass" fibres coated with silane with a nominated length of 4.5 mm were manufactured by Nippon Electronic Glass. The average diameter of the fibres was 13 µm. A knife-mill grinder was used to reduce the average fibre length down to 1 mm. Polypropylene-g-maleic anhydride with a maleic anhydride content of 8 to 10 wt.% and a density of 0.9 g/cm³ was purchased from Sigma-Aldrich®. Four PP_Rmx%/GF composites with 10 wt.% short glass fibres (as proposed in [14]) and different PP-g-MA contents were prepared using melt-mixing. Particularly, the polymer matrix was modified using $x = 0, 0.5, 1$ and 2.5 wt.% of PP-g-MA. PP_R was melt-mixed alongside the PP-g-MA and the glass fibres in a *co*-rotating, twin-screw roller blade Haake-Buchler using a mixing temperature

of 190 °C. The melts were mixed for a total time of 15 min using a rotation speed of 30 rpm. Afterwards, the melts were taken out the rheomixer and left to rest and reach room temperature. The composites were then chopped manually into granules with a size of approximately 2 mm × 1 mm.

2.2. Composite Specimen Preparation and Characterization

The crystalline structure and crystallinity of the composites was tested using a two-circle Rigaku Ultima⁺ diffractometer employed with a Cu-K α X-ray radiation source. Thin polymeric films suitable for X-ray diffraction (XRD) characterization were prepared for each sample using a Paul-Otto Weber type PW 30 hydraulic press operating at 190 °C. The press operation temperature was controlled by an Omron E5AX Temperature Controller. The polymeric granules were hot-pressed for two minutes using a pressure of 80 kN, forming films of approximately 200 μ m thickness. After melting, the formed films were cooled down at RT using a cool water sink.

The melting and cooling behaviour of the composites was investigated using differential scanning calorimetry (DSC, Netzsch DSC 214 Polyma, Germany) under a N₂ flow of 60 mL/min. All specimens underwent a thermal history erase procedure during which the temperature rose up to 200 °C and then reduced down to 20 °C. The thermograms were obtained by heating up the samples at 180 °C and then cooling down to 20 °C. The heating/cooling rate for both the thermal history erase and thermogram recording was 15 °C/min. For the glass transition measurements, the samples were initially heated up to 200 °C using a heating rate of 20 °C/min, rapidly cooled down to –100 °C using a cooling rate of 150 °C/min and then warmed up again using a rate of 20 °C/min.

Tensile mechanical tests were conducted using dumbbell-shaped specimens characterized by an overall length and width of 38 mm and 1.6 mm, respectively. Tests were performed according to the ASTM D638 standard using an Instron Model 3344 2 kN capacity dynamometer and applying a crosshead speed of 50 mm/min. The dynamometer was controlled using Instron Bluehill for Windows 2000. The average Young's modulus, yield strength and stress at break-point values, which were then used to calculate the elongation at break, were obtained after testing five specimens for each sample. The hot press was employed to melt the granules and form approximately 1 mm thick films, which were then cut into suitable specimens using a Wallace S1 cutting press operated by hand.

Dynamic mechanical analysis (DMA) was also carried out on rectangular specimens (span length 40 mm, width 12 mm and height 4 mm) using a PerkinElmer Diamond DMA (PerkinElmer Inc., Wellesley, MA, USA). DMA bending characterization was performed over the temperature range of 25 to 110 °C, using a 3 °C/min heating rate, a bending force of 4000 mN and an oscillation frequency of 1 Hz. The maximum amplitude was set at 10 μ m, while N₂ (>99.9%) was purging the oven constantly at a 20 mL/min flow rate. DMA specimens were formed using the press and suitable metallic moulds.

Scanning electron microscopy (SEM) observation of the tensile specimens' fracture surfaces was carried out using a JEOL JSM 840A-Oxford ISIS 300 SEM, Tokyo, Japan (20 kV).

3. Results and Discussion

The crystalline phase and crystallinity percentage of PP_R, PP-g-MA and the PP_Rm_x%/GF composites were determined using the wide-scan X-ray diffraction patterns shown in Figure 1. All patterns demonstrated strong crystalline diffraction peaks at 2 θ angles of approximately 14.1°, 16.8°, 18.4° and 21.2°, which are typical for the monoclinic alpha crystal phase of polypropylene. It is apparent that the modification of the PP_R matrix using PP-g-MA did not affect the form of the diffraction pattern; however, the crystallinity percentage of the composites is different compared to that of neat PP_R. Table 1 summarizes

the effect of glass fibres and the various content of PP-g-MA on the crystallinity of PP_R. The crystallinity index I_c of the samples was calculated using the equation [15]:

$$I_c = \left(\frac{A_{\text{cryst.}}}{A_{\text{tot.}}} \right) \times 100\% \quad (1)$$

where A_{cryst.} is the integrated area of the crystalline peaks of the diffraction pattern, and A_{tot.} is the total integrated area, namely the area under the crystalline peaks and the amorphous hallow.

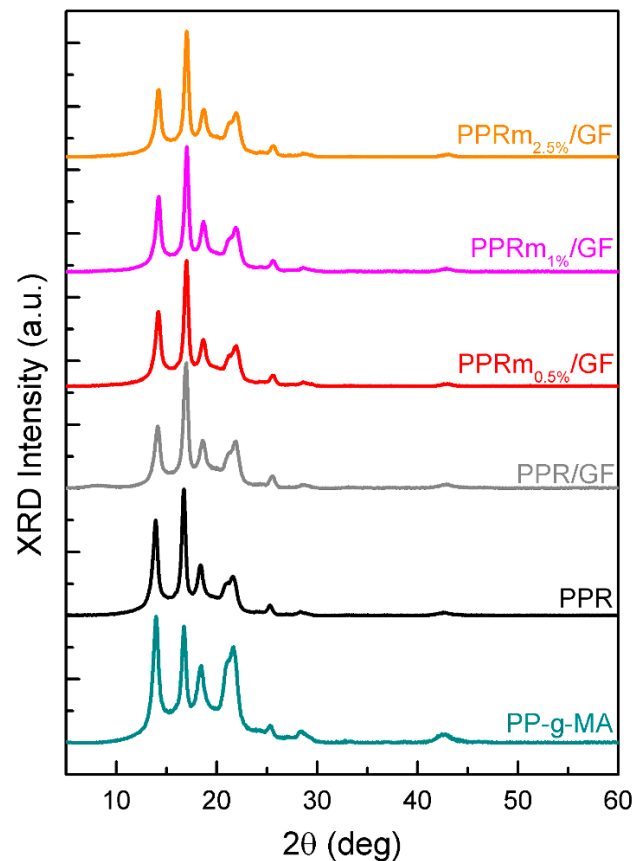


Figure 1. X-ray diffraction pattern of PP_R-, PP-g-MA- and PP-g-MA-treated glass-fibre-reinforced PP_R composites.

Table 1. Crystalline structure characteristics of PP_R, PP-g-MA and the PP_Rm_x%/GF composites.

Sample	Crystallinity, I _c (%)
PP _R	62.1
PP-g-MA	59.2
PP _R m ₀ %/GF	55.5
PP _R m _{0.5} %/GF	54.7
PP _R m ₁ %/GF	52.9
PP _R m _{2.5} %/GF	53.1

The crystallinity of the PP-g-MA compatibilizer is slightly lower compared to PP_R due to the lower molecular weight of the grafted polypropylene, as well as due to the branched MA groups. As for the crystallinity index of the composites, the incorporation of 10 wt.% glass fibres in the matrix without the addition of the compatibilizer significantly lowered the crystallinity from 62.1 to 55.5%. This is due to interruption of the linear crystallization of the PP_R chains during cooling as a result of the random distribution of the GFs in the matrix, which leads to an increase in the amorphous content [16]. The crystallinity of the

PPR_{m_x%}/GF composites is about the same as that of the non-modified material PPR_{m₀%}/GF, indicating that modifying the PPR with the addition of up to 2.5 wt.% PP-g-MA does not significantly decrease the ability of PPR to crystallize [17]. The crystallinity values decrease as the modification increases, reaching 53% for PPR_{m₁%}/GF and PPR_{m_{2.5}%}/GF.

Following the XRD analysis, it is apparent that the amorphous content in the composites varies from 38 to 47%. It is thus expected that the amorphous fraction is enough to demonstrate a glass transition temperature (T_g). The glass transition of the samples was tested using differential scanning calorimetry. Figure 2a presents the heat flow curves obtained for the PPR matrix and the fibre reinforced modified composites on a narrow temperature range around the T_g . The glass transition was calculated using the midpoint temperature method [18]. Figure 2b shows the glass transition temperature dependence on the addition of glass fibres and different PP-g-MA content in the PPR matrix. The addition of glass fibres and the compatibilizer resulted in a drop in T_g temperature, indicating an overall improvement in the polymer chain mobility and the existence of fibre/matrix and/or fibre/fibre slipping and sliding interaction mechanisms [19,20]. The addition of up to 2.5 wt.% PP-g-MA slightly increased T_g from -11.3 °C for composite PPR_{m₀%}/GF to -10.2 °C for PPR_{m_{2.5}%}/GF due to the improved interfacial adhesion between the glass fibres and the PPR matrix, resulting in refined interfaces. However, it is noted that the addition of a small amount of compatibilizer only slightly enhanced the fibre/matrix interaction.

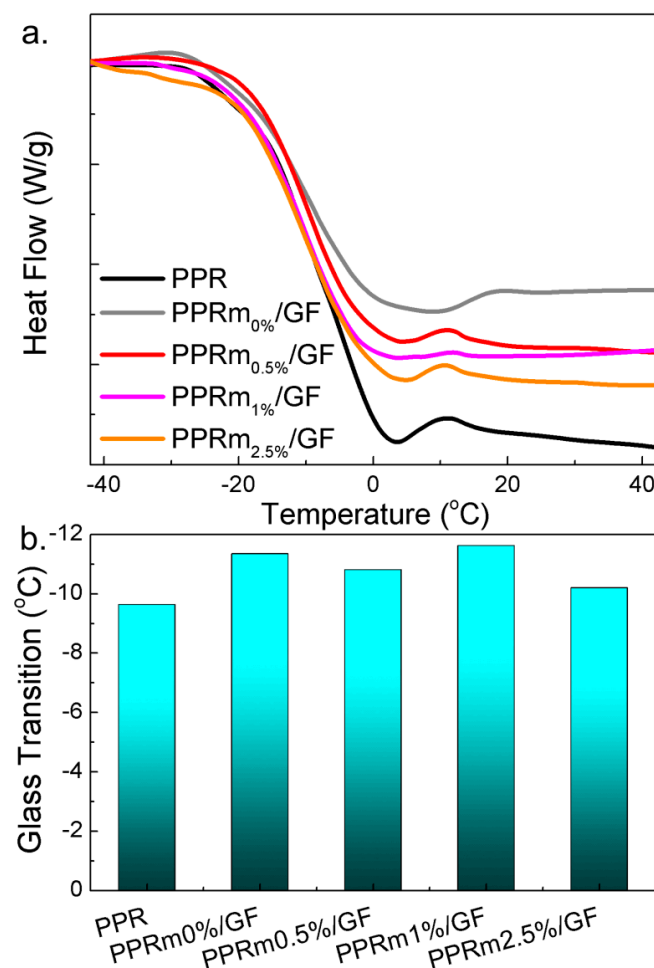


Figure 2. (a) DSC heat flow curves of neat PPR and the PPR_{m_x%}/GF composites focused on the temperature range close to the glass transition. (b) Glass transition temperature is calculated using the midpoint method. The measurements were performed in nitrogen flow of 60 mL/min using a heating rate of 20 °C/min.

The melting and crystallization properties of the samples were also tested using DSC. Figure 3 shows the thermograms of neat PPR and the PPR_mx%/GF composites obtained following the thermal history erase procedure. Single melting and crystallization peaks obtained for all samples confirmed the single-phase crystalline state of PPR prior to and after the PP-g-MA modification. Table 2 summarizes the effect of glass fibres and different compatibilizer content on the melting and crystallization behaviour of PPR.

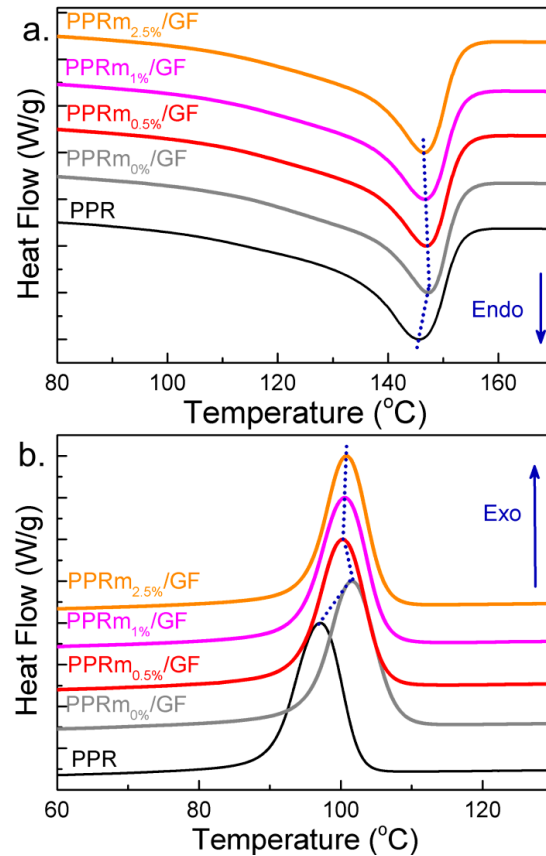


Figure 3. DSC (a) melting and (b) crystallization curves of the PPR and the PPR_mx%/GF composites. The dotted lines are guides to indicate the shift of the DSC melting/crystallization peaks.

Table 2. Melting and crystallization characteristics of neat PPR and glass fibre composites with different compatibilizer content.

Sample	T _m (°C)	T _c (°C)	ΔH _m (J/g)	ΔH _c (J/g)
PPR	145.7	97.1	61.7	65.0
PPR _m 0%/GF	147.2	101.6	52.9	55.2
PPR _m 0.5%/GF	146.9	100.3	53.3	57.2
PPR _m 1%/GF	146.7	100.6	52.7	56.0
PPR _m 2.5%/GF	146.6	100.8	51.1	55.5

Incorporation of 10 wt.% glass fibres in the PPR significantly enhanced the crystallization temperature from 97.1 to 101.6 °C, suggesting the heterogeneous nucleation of PP on the surface of the fibres, leading to faster crystallization rates [14,21]. The addition of PP-g-MA in the PPR/GF composites also resulted in slightly lower melting and crystallization temperatures, while the effect on the melting enthalpy (ΔH_m) is only marginal. The determined values of the crystallization enthalpy (ΔH_c) are higher compared to that of PPR_m0%/GF composite because of the improved compatibility between the fibres and PPR. It is also noted that with an increment to the compatibilizer content, the melting temperature, the melting enthalpy and the crystallization enthalpy decreased slightly, indicating

the limited effect PP-g-MA on the interaction mechanism of the PP_R/GF interfaces and the nucleation of PP_R [22]. This confirms the glass transition temperature results discussed earlier. Furthermore, it is expected that with the lowering of the crystallization enthalpy, the crystallinity will also be reduced, and the composites will become less brittle, which is in excellent agreement with the results obtained for the XRD crystallinity index.

Tensile testing stress–strain curves until fracture were obtained for all samples. The recorded stress–strain curves were used to calculate the elongation percentage at break-point, the yield strength and the Young’s modulus (E), and the results are shown in Table 3. The use of glass fibres resulted in a considerable increment of the elastic modulus from 194 for neat PP_R to 481 MPa for the PP_Rm_{0%}/GF composites, as a result of the effective stiffening effect of GFs to the PP_R matrix. The reinforcing effect of the glass fibres becomes more evident when the compatibilizer is incorporated in the composite, confirming once more the improvement of the matrix/fibre interaction with the addition of PP-g-MA [23]. Incorporation of up to 2.5 wt.% of PP-g-MA provided a hardening contribution, and the Young’s modulus increased to 532 MPa. It is no wonder, despite the small ratio, since a satisfactory adhesion facilitates GF to provide mechanical endurance, by transferring the load to the polymeric matrix. The effect of the fibres and compatibilizer content on the Young’s modulus of the PP_R matrix was also analysed using the Halpin–Tsai equation [24]:

$$E_c = E_m \left(\frac{1 + \zeta \eta V_f}{1 - \eta V_f} \right) \quad (2)$$

where E_m and E_c are the Young’s modulus of PP_R and the PP_Rm_{x%}/GF composites, respectively, $V_f = 0.037$ is the volume fraction of the 10 wt.% glass fibres in the composites and ζ is the reinforcing parameter. The parameter η can be calculated using the equation:

$$\eta = \frac{E_f - E_m}{E_f + \zeta E_m} \quad (3)$$

where $E_f = 80$ GPa is the Young’s modulus value of the glass fibres [25]. The PP_R matrix modulus was found equal to 194 MPa. The reinforcing efficiency can take a large range of values, $0 \leq \zeta \leq \infty$, depending on the matrix, the fillers, the fibre packaging, the isotropy of the system, etc. For very small ζ values, the composite is considered to be stress-loaded in the direction transverse to that of the fibres’ direction, whereas for large ζ values, the stress is considered to be applied parallel to the fibres [24]. Various ζ parameter values were used to describe the Young’s modulus of the composites, as shown in Table 3. The PP_Rm_{x%}/GF demonstrated a reinforcing efficiency varying approximately from 40 to 60, indicating similar fibre spatiality. The small increase in ζ values with the addition of the compatibilizer can be attributed to the improved fibre/matrix interaction as well as the reduced fibre/fibre interactions due to the PP-g-MA “lubrication”. This means that the addition of PP-g-MA in the composites limits the fibre interaction during processing, avoiding fibre breakage and the shrinking of the fibres’ length. As a result, an improved load-bearing capacity and stiffening is achieved due to the sufficient length of the fibres facilitating stress transfer [26]. The yield point of tensile strength of the composites shows similar behaviour to the modulus as a result of the good stress transfer. A maximum value of 26 MPa was obtained for PP_Rm_{1%}/GF. However, as the yield strength values and their deviation for the PP_Rm_{1%}/GF and PP_Rm_{2.5%}/GF composites are comparable, clear conclusions cannot be obtained for these data. Even though the use of a compatibilizer allows the application of higher stress loads before the irreversible deformation starts, the maximum failure stress and thus the elongation at break significantly decreased for the composites. Tröltzsch et al. [27] observed lowering of the load-bearing capability of the composites, which can be attributed to the formation of intermolecular hydrogen bonds due to the presence of the compatibilizer. H-bonds are weaker than covalent bonds, but they add affinity and “collision” if present in a system.

Table 3. The tensile strength, Young's modulus (E), elongation at break and reinforcing parameter (ζ) values of neat PP_R and the $PP_{Rm_x\%}/GF$ composites (mean \pm sd. and $n = 5$, where n is the number of specimens).

Sample	Young Modulus (MPa)	Reinforcing Parameter, ζ	Yield Strength (MPa)	Elongation at Break (%)
PP_R	194 ± 16	-	17 ± 3	761 ± 89
$PP_{Rm0\%}/GF$	481 ± 39	42	23 ± 1	627 ± 43
$PP_{Rm0.5\%}/GF$	496 ± 49	44	23 ± 2	604 ± 45
$PP_{Rm1\%}/GF$	508 ± 35	58	26 ± 4	600 ± 39
$PP_{Rm2.5\%}/GF$	532 ± 54	50	24 ± 2	578 ± 32

Figure 4 shows SEM images obtained from the fracture surface of the tensile test specimens of the samples. As shown in Figure 4a, the fracture surface of pure PP_R is smooth with a granular appearance without any sign of plastic deformation, characteristics of a brittle fracture. The incorporation of glass fibres in the random polypropylene matrix (Figure 4b,c) led to the breakage and withdrawal of the fibres at the fracture point during the elongation. The GFs appear peeled off the PP_R (Figure 4c, white arrows) due to the pure fibre/matrix adhesion, while the polymeric matrix demonstrated a fibrillar-like structure (Figure 4b), possibly related to the local plastic deformation of PP_R . Previous publications suggest that the fibrillation of the matrix is due to the enhancement of plastic deformation around the glass fibres [28]. Furthermore, the bare glass fibres seem to have a certain degree of orientation possible due to a fibre twist, which occurred in the matrix during the elongation stress loading.

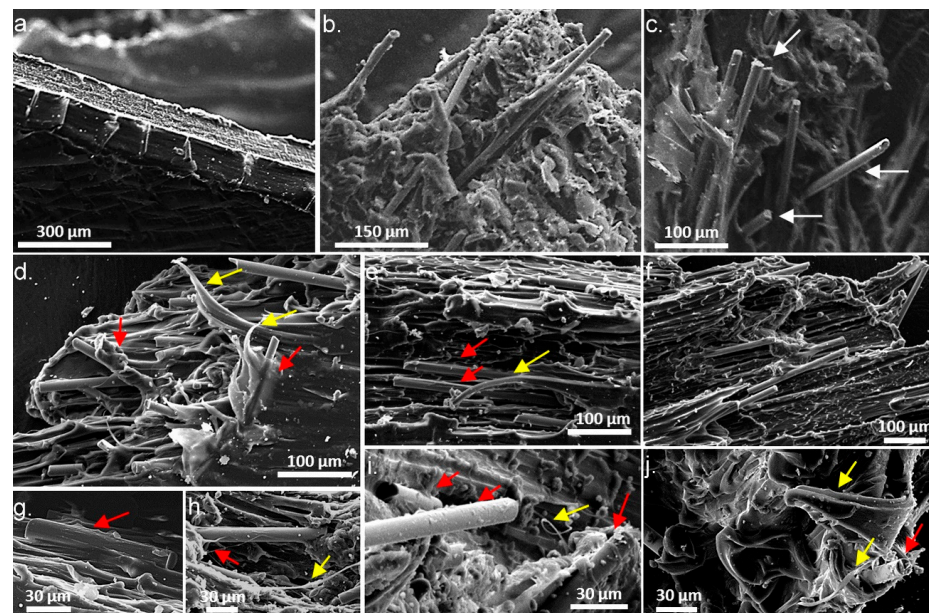


Figure 4. SEM images obtained for the fracture surface of (a) the neat PP_R , (b,c) the $PP_{Rm0\%}/GF$, (d) $PP_{Rm0.5\%}/GF$, (e) $PP_{Rm1\%}/GF$ and (f) the $PP_{Rm2.5\%}/GF$. Higher resolution SEM images of (g,h) the $PP_{Rm0.5\%}/GF$, (i) the $PP_{Rm1\%}/GF$ and (j). White arrows—neat GF, red arrows—GF with adhered polymer matrix, yellow arrows—fibrillar matrix.

For the PP-g-MA $PP_{Rm2.5\%}/GF$ modified composites, the matrix demonstrated an extended plastic deformation and higher fracture surface roughness due to extensive fibrillar formations (yellow arrows in Figure 4d,e,h-j). Additionally, it is apparent that the addition of the compatibilizer in the composites improved the PP_R matrix adhesion on the fibres. The GFs present at the fracture surface were mostly covered by a polymer layer (red arrows in Figure 4d,g). Alternatively, PP_R fractions of various dimensions were well attached on the surface of the fibres (red arrows in Figure 4h-j). The improvement of the

bonding capability of the matrix on the glass fibre surface due to formation of chemical bonds promoted by the addition of PP-g-MA enables transferring of the applied strain load from the matrix to the fibres, leading to higher Young's modulus and yield strength values as discussed earlier. Furthermore, the improvement of the ductility of the $PP_{Rm_x\%}/GF$ composites is considered the main failure mechanism lowering the maximum stress the composites can withstand during flexural tests before breaking and as a result the lower elongation at break (Table 3) [28].

Finally, the effect of the addition of a compatibilizer on the thermomechanical properties of the composites was also tested using dynamic mechanical analysis (DMA). Figure 5 shows the temperature dependence of the storage modulus, E' , and the ratio of loss to storage modulus, $\tan\delta$, at a frequency of 1 Hz of all the samples. Up to approximately 60 °C, the storage modulus of all samples demonstrates a sharp decrease due to the relaxation of the amorphous phase that follows the glass transition region. Furthermore, with the addition of the glass fibres and the compatibilizer, the storage modulus increases throughout the temperature range studied. In particular, the $PP_{Rm_0\%}/GF$ composite demonstrated an increase measuring from 10 to 32% in the modulus compared to neat PP_R , while the addition of the compatibilizer resulted in a maximum modulus approximately 1.3 times higher for the $PP_{Rm_{2.5\%}}/GF$ composite compared to the non-modified composite. Despite seeming a bit inconsistent, $\tan\delta$ curves are in accordance with the literature for PP for recordings above RT [29].

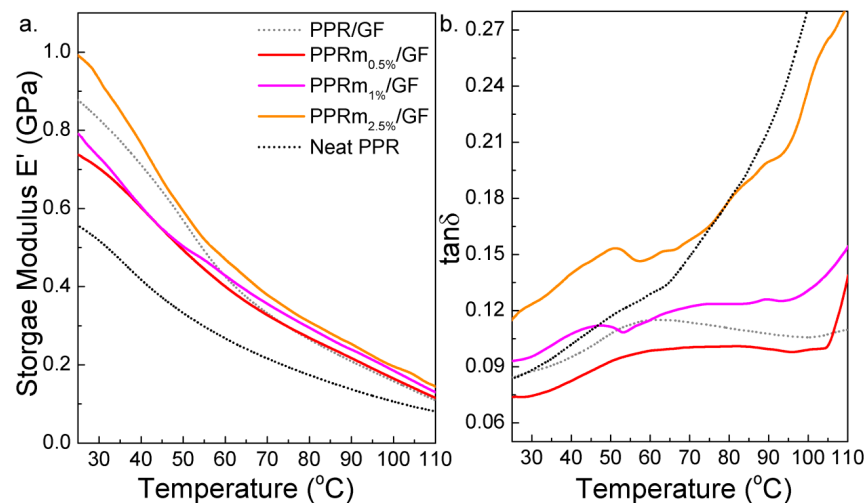


Figure 5. (a) Storage modulus E' and (b) $\tan\delta$ curves of neat PP_R and the $PP_{Rm_x\%}/GF$ composites as a function of temperature.

The storage modulus improvement over the experimental temperature range confirms the improved stiffening and reinforcing effect of the fibres due to the addition of the modifier, typical of the enhanced fibre/matrix interaction. Overall, the $\tan\delta$ decreases with the addition of fibres in the PP_R matrix due to the moderate interaction between the polymeric matrix and the fillers. Incorporation of the modifier improved the energy dissipation potential of the composites; however, only $PP_{Rm_{2.5\%}}/GF$ demonstrated similar vibration damping efficiency to neat PP_R . The rest of the composites exhibited a rather elastic character, which is expected to improve the load storage capacity of the PP_R matrix. Furthermore, the irregularity in $\tan\delta$ curves of $PP_{Rm_1\%}/GF$ and $PP_{Rm_{2.5\%}}/GF$ shown at 55–60 °C is rather attributed to displacement of some rigid parts of the polymeric chains, perhaps because of the preparation mixing process.

4. Conclusions

In summary, reinforced PP_R composites with 10 wt.% short glass fibres were prepared using melt-mixing. PP-g-MA was added in the composites as a means to improve the

PP_R matrix/fibre interaction and the thermomechanical characteristics of the composites. The effect of the glass fibre and compatibilizer addition on the structural, thermal and mechanical properties of the composites was investigated. Analysis of the XRD patterns of the samples indicated a strong drop in the crystallinity index upon the addition of the fibres due their random distribution in the matrix, which limits the formation of long PP_R chains. DSC characterization suggested that the fibres acted as nucleation agents promoting the faster crystallization during cooling, while the addition of PP-g-MA only marginally affected the crystallization of the composites. Furthermore, the improved PP_R matrix/fibre adhesion significantly enhanced the flexural strength of the composites, resulting in a maximum Young's modulus. SEM imaging of the surface fracture of the samples also confirmed the matrix attachment on the fibres with the addition of the compatibilizer, while the fibrillar appearance of the matrix indicated its plastic deformation. Finally, the addition of the compatibilizer has shown increase in the storage modulus due to the improved adhesion between the PP_R matrix and the surface of the glass fibres. Also, the addition of the fibres greatly reduced the dissipation potential of the matrix, while the loss tangent was not significantly affected for a PP-g-MA content up to 1 wt.%, as indicated by the DMA findings. These results revealed the synergistic effect of the glass fibres and the PP-g-MA compatibilizer on enhancing the crystallization, stiffness, strength and storage modulus of PP_R. This confirms the prospect of forming advanced glass-fibre-reinforced PP_R composites with improved matrix/fibre interaction characteristics appears suitable for a broad range of commercial applications such as water supply pipelines, by incorporating small amount of compatibilizer, without significantly raising the production cost, making it an industrial feasible strategy.

Author Contributions: Conceptualization, K.C. and D.B.; methodology, E.D. and D.G.; software, E.D. and E.V.; validation, E.D. and D.G.; investigation, E.D. and E.V.; data curation, E.D.; writing—original draft preparation, E.D. and E.V.; writing—review and editing, D.B. and E.V.; supervision, K.C.; project administration, K.C.; funding acquisition, K.C. All authors have read and agreed to the published version of the manuscript.

Funding: This work was financially supported by Greek national funds alongside the Regional Development Fund of the European Union through the operational program Competitiveness, Entrepreneurship and Innovation (research call RESEARCH—CREATE—INNOVATE, code of the project: T1EDK-02575). The authors would also like to thank C. Papoulia, E. Pavlidou and G. Vourlias (AMDe Lab, Department of Physics, Aristotle University of Thessaloniki) for their support.

Data Availability Statement: The data presented in this study are available on request from the corresponding author (accurately indicate status).

Conflicts of Interest: The authors declare no conflicts of interest.

References

1. Sathishkumar, T.P.; Satheshkumar, S.; Naveen, J. Glass fiber-reinforced polymer composites—A review. *J. Ren. Plast. Comp.* **2014**, *33*, 1258–1275. [[CrossRef](#)]
2. Zaman, I.; Manshoor, B.; Khalid, A.; Araby, S. From clay to graphene for polymer nanocomposites—A survey. *J. Polym. Res.* **2014**, *21*, 429. [[CrossRef](#)]
3. Hagnell, M.K.; Åkermo, M. The economic and mechanical potential of closed loop material usage and recycling of fibre reinforced composite materials. *J. Clean. Prod.* **2019**, *223*, 957–968. [[CrossRef](#)]
4. Thomason, J.L. Glass fibre sizing: A review. *Compos. Part A* **2019**, *127*, 105619. [[CrossRef](#)]
5. Etcheverry, M.; Barbosa, S.E. Glass fiber reinforced polypropylene mechanical properties enhancement by adhesion improvements. *Materials* **2012**, *5*, 1084–1113. [[CrossRef](#)] [[PubMed](#)]
6. Kim, H.I.; Han, W.; Choi, W.K.; Park, S.J.; An, K.H.; Kim, B.J. Effects of maleic anhydride content on mechanical properties of carbon fibers-reinforced maleic anhydride-grafted-poly-propylene matrix composites. *Carbon Lett.* **2016**, *20*, 39. [[CrossRef](#)]
7. Zheng, A.; Wang, H.; Zhu, X.; Masuda, S. Studies on the interface of glass fiber-reinforced polypropylene composite. *Comp. Interfaces* **2002**, *9*, 319–333. [[CrossRef](#)]
8. Rijdsdijk, H.A.; Contant, M.; Peijs, A.A.J.M. Continuous-glass-fibre-reinforced polypropylene composites: I. influence of maleic-anhydride-modified polypropylene on mechanical properties. *Comp. Sci. Technol.* **1993**, *48*, 161–172. [[CrossRef](#)]

9. Ismail, H.; Nordin, R.; Ahmad, Z.; Rashid, A. Processability and miscibility of linear low-density polyethylene/poly (vinyl alcohol) blends: In situ compatibilization with maleic acid. *Iran. Polym. J.* **2010**, *19*, 297–308.
10. Van der Wall, A.; Nijhof, R.; Gaymans, R.J. Polypropylene-rubber blends: 2. The effect of the rubber content on the deformation and impact behavior. *Polymer* **1999**, *40*, 6031–6044. [[CrossRef](#)]
11. Pereira, J.R.D.; Bemardes, G.P.; Silva, J.A.P.; Bönmann, V.C.; Calcagno, C.I.W.; Santana, R.M.C. Structure-property correlation of an impact-modified random polypropylene copolymer. *J. Elastom. Plastics.* **2020**, *53*, 450–468. [[CrossRef](#)]
12. Ou, C.F. The crystallization characteristics of polypropylene and low ethylene content polypropylene copolymer with copolyesters. *Eur. Pol. J.* **2002**, *38*, 467–473. [[CrossRef](#)]
13. Li, Y.; He, S.; He, H.; Yu, P.; Wang, D. Study on low temperature toughness and crystallization behavior of polypropylene random copolymer. *J. Polym. Eng.* **2017**, *37*, 715–727. [[CrossRef](#)]
14. Delli, E.; Giliopoulos, D.; Bikiaris, D.N.; Chrissafis, K. Fibre length and loading impact on the properties of glass fibre reinforced polypropylene random composites. *Comp. Struct.* **2021**, *263*, 113678. [[CrossRef](#)]
15. Kim, H.S.; Lee, B.H.; Choi, S.W.; Kim, S.; Kim, H.J. The effect of types of maleic anhydride-grafted polypropylene (MAPP) on the interfacial adhesion properties of bio-flour-filled polypropylene composites. *Compos. Part A* **2007**, *38*, 1473–1482. [[CrossRef](#)]
16. Hassan, A.; Rahman, N.A.; Yahya, R. Extrusion and injection-molding of glassfiber/MAPP/polypropylene: Effect of coupling agent on DSC, DMA, and mechanical properties. *J. Reinf. Plast. Compos.* **2012**, *30*, 1223–1232. [[CrossRef](#)]
17. Wang, Y.; Shi, Y.; Shao, W.; Ren, Y.; Dong, W.; Zhang, F.; Liu, L.Z. Crystallization, structures, and properties of different polyolefins with similar grafting degree of maleic anhydride. *Polymers* **2020**, *12*, 675. [[CrossRef](#)] [[PubMed](#)]
18. Curtzwiler, G.; Early, M.; Gottschalk, D.; Konecki, C.; Peterson, R.; Wand, S. The world of surface coatings is centered around the: Glass transition temperature, but which one? Part 1. *JCT Coat. Technol.* **2004**, *11*, 28.
19. Lopez-Manchado, M.A.; Biagiotti, J.; Kenny, J.M. Comparative Study of the Effects of Different Fibers on the Processing and Properties of Polypropylene Matrix Composites. *J. Therm. Comp. Mater.* **2002**, *15*, 337–353. [[CrossRef](#)]
20. Nimmagadda, P.B.R.; Sofronist, P. On the calculation of the matrix-reinforcement interface diffusion coefficient in diffusional relaxation of composite materials at high temperatures. *Acta Mater.* **1996**, *44*, 2711–2716. [[CrossRef](#)]
21. Amash, A.; Zugenmaier, P. Thermal and dynamic mechanical investigations on fiber-reinforced polypropylene composites. *J. Appl. Polym. Sci.* **1997**, *63*, 1143–1154. [[CrossRef](#)]
22. Renaut, N.; Duquesne, S.; Zanardi, S.; Bardollet, P.; Steil, C.; Delobel, R. Fire retardancy, thermomechanical and thermal properties of PP/PC blends. *J. Macromol. Sci. Part A Pure Appl. Chem.* **2005**, *42*, 977–991. [[CrossRef](#)]
23. Zhai, Z.; Liu, Z.; Feng, L.; Liu, S. Interfacial adhesion of glass fibre reinforced polypropylene–maleic anhydride modified polypropylene copolymer composites. *J. Reinf. Plast. Compos.* **2014**, *33*, 785–793. [[CrossRef](#)]
24. Osoka, E.A.; Onukwuli, O.D. A modified Halpin-Tsai model for estimating the modulus of natural fiber reinforced composites. *Int. J. Eng. Sci. Invent.* **2018**, *7*, 63–70.
25. Hara, S.; Watanabe, S.; Takahashi, K.; Shimizu, S.; Ikake, H. Preparation of crystallites for oriented poly(lactic acid) films using a casting method under a magnetic field. *Polymers* **2018**, *10*, 1083. [[CrossRef](#)]
26. Van den Oever, M.; Peijs, T. Continuous-glass-fibre-reinforced polypropylene composites: II. Influence of maleic-anhydride modified polypropylene on fatigue behavior. *Compos. Part A* **1998**, *29A*, 227–239. [[CrossRef](#)]
27. Tröltzsch, J.; Stiller, J.; Hase, K.; Roth, I.; Helbig, F.; Kroll, L. Effect of maleic anhydride modification on the mechanical properties of a highly filled glass fibre reinforced, low-viscosity polypropylene for injection moulding. *J. Mater. Sci. Res.* **2016**, *5*, 111–120.
28. Schoßig, M.; Zankel, A.; Bierögel, C.; Pölt, P.; Grellmann, W. ESEM investigations for assessment of damage kinetics of short glass fibre reinforced thermoplastics—Results of in situ tensile tests coupled with acoustic emission analysis. *Comp. Sci. Technol.* **2011**, *71*, 257–265. [[CrossRef](#)]
29. Brylka, B.; Schemmann, M.; Wood, J.; Böhlke, T. DMA based characterization of stiffness reduction in long fiber reinforced polypropylene. *Polym. Test.* **2018**, *66*, 296–302. [[CrossRef](#)]

Disclaimer/Publisher’s Note: The statements, opinions and data contained in all publications are solely those of the individual author(s) and contributor(s) and not of MDPI and/or the editor(s). MDPI and/or the editor(s) disclaim responsibility for any injury to people or property resulting from any ideas, methods, instructions or products referred to in the content.